

RESEARCH PAPER

## Facile Preparation of Silver Nanoparticles and Antibacterial Chitosan-Ag Polymeric Nanocomposites

Ziba Sorinezami <sup>1,\*</sup>, Davood Ghanbari <sup>2</sup>

<sup>1</sup> Department of Chemistry, Faculty of Science, University of Zabol, Zabol, Iran

<sup>2</sup> Department of Science, Arak University of Technology, Arak, Iran

### ARTICLE INFO

#### Article History:

Received 04 March 2019

Accepted 17 May 2019

Published 01 July 2019

#### Keywords:

Antibacterial

Chitosan

Nanocomposite

Nanostructures

Silver

### ABSTRACT

Silver nanostructures as an effective antibacterial materials were synthesized via three various hydrothermal, sono-chemical and microwave methods using water as a green solvent. Then Chitosan-Ag polymer based nanocomposites were made by a fast chemical procedure. The influence of power, temperature and time on the morphology and particle size of the products was investigated. Scanning electron microscopy (SEM) approved that mono-disperse nanoparticles were achieved using all three procedures. X-ray diffraction (XRD) and Fourier transform infrared (FT-IR) spectroscopy confirmed preparation of pure products. The antibacterial behaviour of Chitosan-Ag nanocomposites was evaluated using degradation of E coli bacteria. The results show a nanocomposite with applicable antibacterial performance in burn wounds.

#### How to cite this article

Sorinezami Z, Ghanbari D. Facile Preparation of Silver Nanoparticles and Antibacterial Chitosan-Ag Polymeric Nanocomposites. J Nanostruct, 2019; 9(3): 396-401. DOI: 10.22052/JNS.2019.03.001

### INTRODUCTION

Chitosan is a linear biomedical polysaccharide and it is made by treating the chitin shells of crustaceans with an alkaline substance in excess as a reagent and water as a solvent. It can be used in agriculture as a seed treatment, bio-pesticide that helps plants to fight off fungal infections, wine making, self-healing polyurethane paint coating, antibacterial bandages and deliver drugs through the skin.. Chitosan is hypoallergenic antibacterial and biodegradable and its derivatives have been used in nonviral gene delivery, transfect breast cancer cells, cytotoxicity; hemostatic agents, pain reducing, transport of polar drugs and treat burn wounds. Chitosan has a positive charge under acidic conditions that comes from protonation of its free amino groups which leads to an increase in solubility [1-7].

Silver nanoparticles have been the subject of extensive research in the frame of nanotechnology, mainly owing to their unique optical properties.

Indeed, the free electron gas of Ag such nanoparticles features a resonant oscillation upon illumination in the visible part of the spectrum. The spectral properties of this resonance depend on the constitutive material, the shape of the nanoparticles and its environment. This resonant electronic oscillation is called localized surface plasmon (LSP), and the field of research that studies the fundamentals and applications of LSP is known as nanoplasmonics. Plasmonic nanoparticles can behave as efficient nanosources of heat, light or energetic electrons, remotely controllable by light [8-11].

Nanostructured silver compounds have achieved great attention, due to their potential applications in different areas of technology such as electronic, sensor, solar cells and photocatalysts. Nano particles with smaller sizes and larger specific surface areas can shorten the diffusion distance of photo generated carriers transferring to the surface of photo catalysts, and

\* Corresponding Author Email: Soori@uoz.ac.ir



increase the surface catalytic active sites [12-15]. In this work Ag and Chitosan-Ag nanocomposites were made by a fast chemical procedure by three applicable hydrothermal, sonochemical and microwaves methods in water as a green solvent.

### MATERIALS AND METHODS

XRD patterns were recorded by a Philips, X-ray diffractometer using Ni-filtered  $\text{CuK}_\alpha$  radiation. SEM images were obtained using a KYKY instrument model EM3200. Prior to taking images, the samples were coated by a very thin layer of Pt (using a BAL-TEC SCD 005 sputter coater) to make the sample surface conductor and prevent charge accumulation, and obtaining a better contrast. A multiwave ultrasonic generator (BandelineMS 73), equipped with a converter/transducer and titanium oscillator, operating at 20 kHz with a maximum power output of 150 W.  $\text{AgNO}_3$ ,  $\text{NaBH}_4$ , starch, glucose, gelatin, poly vinyl pyrrolidone and acetone were purchased from Merck or Aldrich and all the chemicals were used as received without further purifications.

#### Synthesis of silver nanoparticles by hydrothermal, microwave and sonochemical methods

1 g of  $\text{AgNO}_3$  was dissolved in 200 ml of deionized water. 10 ml of  $\text{NaBH}_4$  solution (1M) was then slowly added to the solution. For hydrothermal method the solution was added to autoclave reaction and it was maintained at 180 °C for 5h. For microwave procedure the solution was

irradiated at 600 W for 5 min. for sonochemical preparation the solution was maintained at 150 W for 30 min until a brown precipitate was then centrifuged and rinsed with distilled water. The obtained precipitate was calcinated at 80°C and its colour goes brown.

#### Synthesis of Chitosan-Ag nanocomposite

1 g of Chitosan was dissolved in 10 ml of deionized water (with addition of 1 ml of acetic acid). Then 1g of  $\text{AgNO}_3$  deionized water was added to the mixture containing Chitosan. After 30 minutes the  $\text{NaBH}_4$  solution was slowly added to the aqueous solution and was stirred for 5 hour. The obtained precipitate was dried at 50°C for 2 hour (Fig. 1).

### RESULTS AND DISCUSSION

The composition of the Chitosan-Ag nanocomposite was investigated. Presence of face centred cubic phase (JCPDS No.:891010, space group: Fm-3m, strong Bragg reflection peaks can be seen which correspond to the (111), (200), (220) and (311) reflections) was confirmed and is illustrated in Fig. 2. The crystalline sizes from Scherrer equation,  $D_c = K\lambda/\beta\cos\theta$ , was estimated,  $\beta$  is the width of the observed diffraction peak at its half maximum intensity, K is the shape factor, which takes a value of about 0.9, and  $\lambda$  is the X-ray wavelength ( $\text{CuK}_\alpha$  radiation, equals to 0.154 nm). The average crystalline size for Ag nanoparticles was found to be about 30 nm respectively.

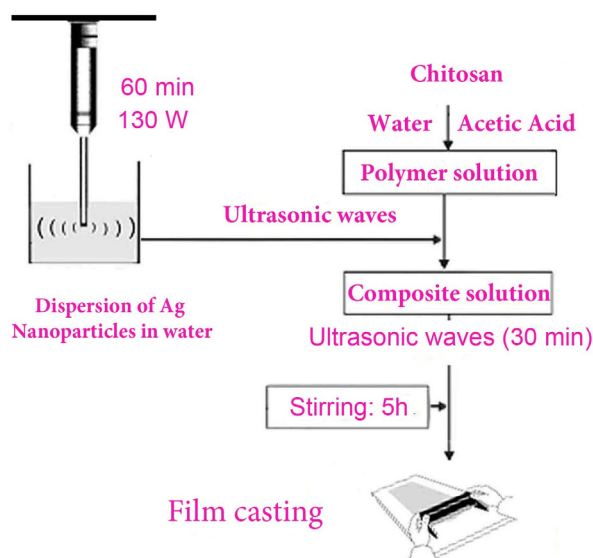


Fig. 1. Schematic of ferrite preparation Chitosan/Ag nanocomposite.

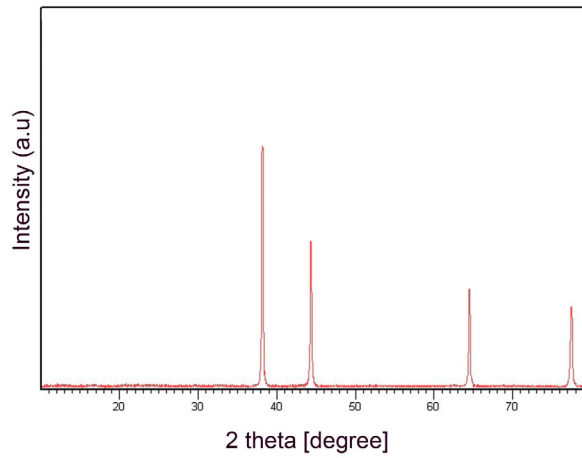


Fig. 2. XRD pattern of Ag nanoparticles.

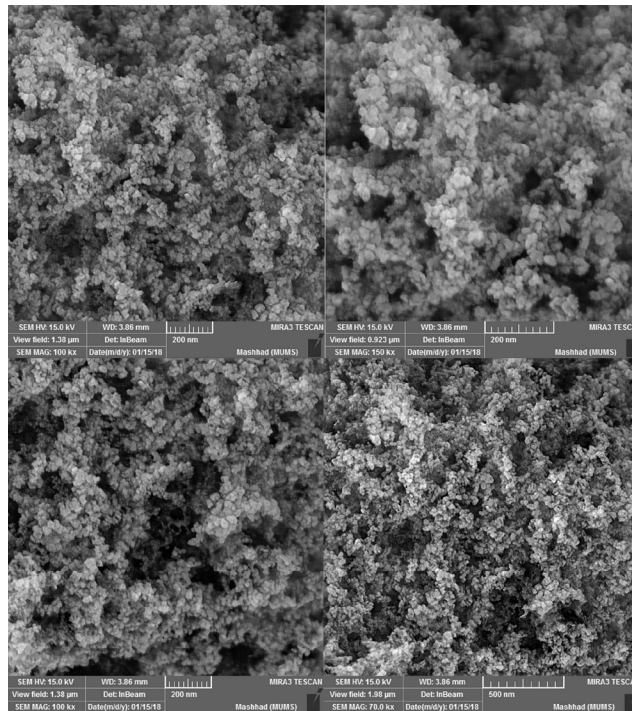


Fig. 3. SEM images of Ag nanoparticles prepared by hydrothermal method

Scanning electron microscopy was employed for estimation of morphology and particle size of the products. Fig. 3. illustrate SEM images of the Ag nanoparticles synthesized by hydrothermal (180 °C, 5h) without using any surfactant and capping that confirm nanostructures were synthesized. The mediocre size was approved about 40 nm. These conditions were chosen as a basic reaction in this work and effect of various parameters was

investigated on the blank reaction.

The influence of microwave waves (600W, 5 min) on the size and shape was also examined, outcomes illustrate by applying microwave at lower reaction times uniform nanoparticles with lower diameter size were prepared (Fig. 4). The average particle size is about 50 nm, results confirm bigger product was prepared in comparison to other products.

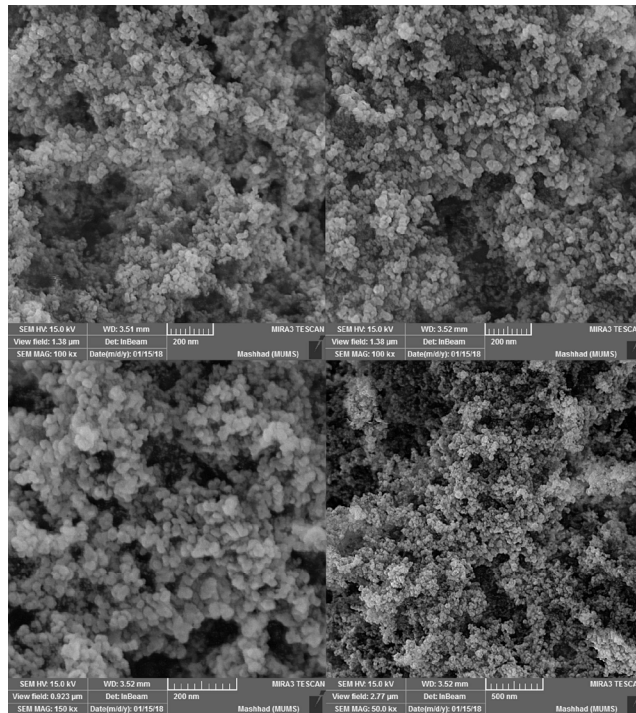


Fig. 4. SEM images of Ag nanoparticles synthesized by microwave method

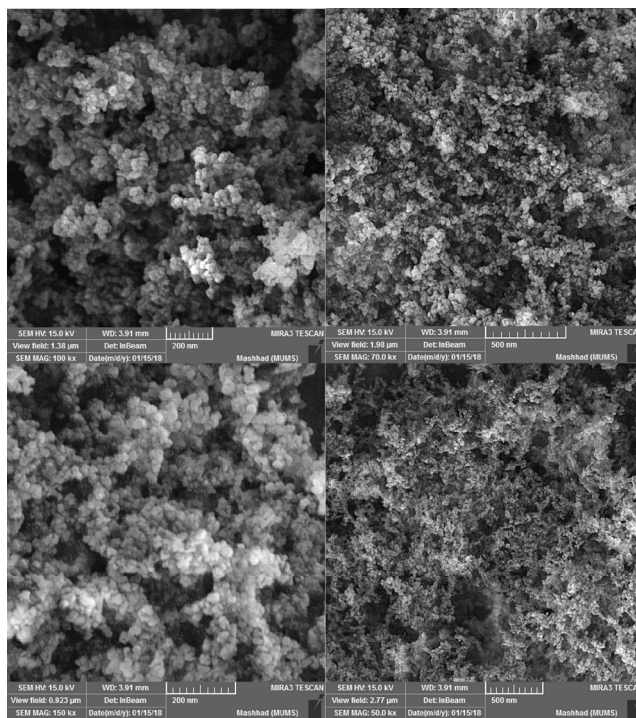


Fig. 5. SEM images of Ag nanoparticles achieved by sonochemical method

Fig. 5 illustrate SEM images of silver nanoparticles prepared by sonochemical (150W, 30 min) the results confirm that also mono-

disperse nanostructure with average size less than 70 nm were synthesized.

Fig. 6. shows the FT-IR spectrum of the as-

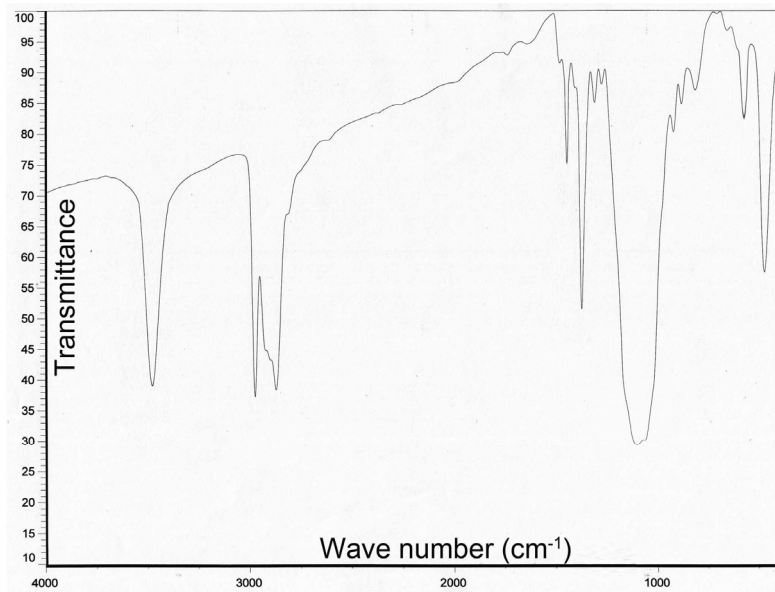


Fig. 6. FT-IR spectrum of Chitosan-Ag nanocomposite.

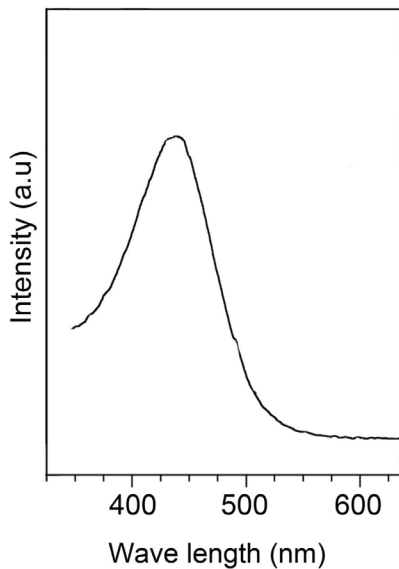


Fig. 7. UV-Vis absorption of chitosan-Ag nanocomposite

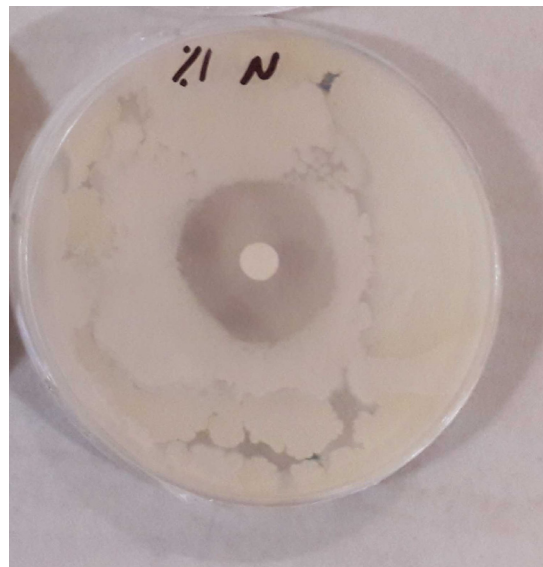


Fig. 8. Antibacterial effect of silver nanoparticles

prepared Chitosan-Ag nanocomposite by applying lemon extract, the absorptions bands at 400-600 $\text{cm}^{-1}$  are assigned to the stretching mode of Ag-O. The spectrum exhibits broad absorption peak around 3300-3400  $\text{cm}^{-1}$ , corresponding to the stretching mode of O-H and N-H bonds. The band near 2900  $\text{cm}^{-1}$  is assigned to C-H vibration mode. Absorption around 1100  $\text{cm}^{-1}$  is related to C-O bonds.

UV-Vis absorption of Ag nanoparticle is shown in Fig. 7. With agreement to previous published

works silver nanoparticles show an absorption around 440 nm. The as-prepared nanocomposite has the potential to be applied to improve environmental problems associated with organic and toxic water pollutants. Antibacterial effect of Chitosan-Ag nanocomposite on the degradation of E Coli bacteria is shown in Fig 8. As time increase; more bacteria are degraded on the nanoparticles catalyst, until obvious circle was observed around antibacterial chitosan-Ag disk.

## CONCLUSIONS

In conclusion, synthesis, characterization and antibacterial activity of Ag and Chitosan-Ag nanocomposites were reported. SEM confirmed that by using three hydrothermal, sonochemical and microwave methods mono-disperse products with bigger sizes were prepared. The antibacterial behaviour of Chitosan-Ag nanocomposite was evaluated using the degradation of E coli bacteria. Maximum absorption peak ( $\lambda_{max}$ ) of silver was observed from UV-vis absorption spectra and has agreement to previous scientific literatures. The results show that these three methods is facile and cost effective method for preparation of Chitosan-Ag nanocomposites as a suitable candidate for antibacterial applications.

## CONFLICT OF INTEREST

The authors declare that there are no conflicts of interest regarding the publication of this manuscript.

## ACKNOWLEDGMENT

This work was funded by University of Zabol Grant No. UOZ-GR-95-7.

## REFERENCES

1. Shahidi F, Synowiecki J. Isolation and characterization of nutrients and value-added products from snow crab (*Chionoecetes opilio*) and shrimp (*Pandalus borealis*) processing discards. *Journal of Agricultural and Food Chemistry*. 1991;39(8):1527-32.
2. Ahlafi H, Moussout H, Boukhilfi F, Echetna M, Bennani MN, My Slimane S. Kinetics of N-Deacetylation of Chitin Extracted from Shrimp Shells Collected from Coastal Area of Morocco. *Mediterranean Journal of Chemistry*. 2013;2(3):503-13.
3. Lee DW, Lim C, Israelachvili JN, Hwang DS. Strong Adhesion and Cohesion of Chitosan in Aqueous Solutions. *Langmuir*. 2013;29(46):14222-9.
4. Lim C, Lee DW, Israelachvili JN, Jho Y, Hwang DS. Contact time- and pH-dependent adhesion and cohesion of low molecular weight chitosan coated surfaces. *Carbohydrate Polymers*. 2015;117:887-94.
5. Kean T, Roth S, Thanou M. Trimethylated chitosans as non-viral gene delivery vectors: Cytotoxicity and transfection efficiency. *Journal of Controlled Release*. 2005;103(3):643-53.
6. Nabiyouni G; Ghanbari D, Fe-Ag nanocomposite: Hydrothermal preparation of iron nanoparticles and silver dendrite like nanostructures . *J Nanostruct*. 2017; 7 (2): 11-120.
7. Khaghani S, Ghanbari D. Magnetic and photo-catalyst Fe<sub>3</sub>O<sub>4</sub>-Ag nanocomposite: green preparation of silver and magnetite nanoparticles by garlic extract. *Journal of Materials Science: Materials in Electronics*. 2016;28(3):2877-86.
8. Masoumi S, Nabiyouni G, Ghanbari D. Photo-degradation of azo dyes: photo catalyst and magnetic investigation of CuFe<sub>2</sub>O<sub>4</sub>-TiO<sub>2</sub> nanoparticles and nanocomposites. *Journal of Materials Science: Materials in Electronics*. 2016;27(9):9962-75.
9. Masoumi S, Nabiyouni G, Ghanbari D. Photo-degradation of Congored, acid brown and acid violet: photo catalyst and magnetic investigation of CuFe<sub>2</sub>O<sub>4</sub>-TiO<sub>2</sub>-Ag nanocomposites. *Journal of Materials Science: Materials in Electronics*. 2016;27(10):11017-33.
10. Nabiyouni G; Ghanbari D; Ghasemi J; Yousofnejad A, Microwave-assisted Synthesis of MgFe<sub>2</sub>O<sub>4</sub>-ZnO Nanocomposite and Its Photo-catalyst Investigation in Methyl Orange Degradation. *J Nanostruct*. 2015; 5 (3): 289-295.
11. Horikoshi S, Serpone N. *Microwaves in nanoparticle synthesis: fundamentals and applications*. John Wiley & Sons. 2013.
12. Asiabani N, Nabiyouni G, Khaghani S, Ghanbari D. Green synthesis of magnetic and photo-catalyst PbFe<sub>12</sub>O<sub>19</sub>-PbS nanocomposites by lemon extract: nano-sphere PbFe<sub>12</sub>O<sub>19</sub> and star-like PbS. *Journal of Materials Science: Materials in Electronics*. 2016;28(1):1101-14.
13. Tompsett GA, Conner WC, Yngvesson KS. *Microwave Synthesis of Nanoporous Materials*. *ChemPhysChem*. 2006;7(2):296-319.
14. Ghanbari D, Salavati-Niasari M. Synthesis of urchin-like CdS-Fe<sub>3</sub>O<sub>4</sub> nanocomposite and its application in flame retardancy of magnetic cellulose acetate. *Journal of Industrial and Engineering Chemistry*. 2015;24:284-92.
15. Ghanbari D, Salavati-Niasari M, Ghasemi-Kooch M. In situ and ex situ synthesis of poly(vinyl alcohol)-Fe<sub>3</sub>O<sub>4</sub> nanocomposite flame retardants. *Particuology*. 2016;26:87-94.